Plant, Cell & Environment

WILEY

Plant, Cell & Environment

ORIGINAL ARTICLE

Root Development of Tomato Plants Infected by the Cacao Pathogen *Moniliophthora perniciosa* Is Affected by Limited Sugar Availability

Daniele Paschoal[1,2] | Laura Cazetta[1,2] | João V. O. Mendes[1,2] | Nathália C. F. Dias[2] | Vitor Ometto[1,2] | Esther Carrera[3] | Mônica L. Rossi[1] | Juliana A. Aricetti[4] | Piotr Mieczkowski[5] | Gabriel G. Carvalho[6] | Igor Cesarino[6,7] | Simone F. da Silva[8] | Rafael V. Ribeiro[8] | Paulo J. P. L. Teixeira[2] | Eder M. da Silva[1] | Antonio Figueira[1]

[1]Centro de Energia Nuclear na Agricultura, Universidade de São Paulo (USP), Piracicaba, São Paulo, Brazil | [2]Escola Superior de Agricultura "Luiz de Queiroz", Universidade de São Paulo (USP), Piracicaba, São Paulo, Brazil | [3]Universitat Politècnica de València (UPV), Consejo Superior de Investigaciones Científicas (CSIC), Valencia, Spain | [4]Laboratório Nacional de Biorrenováveis, Centro Nacional de Pesquisa em Energia e Materiais, Campinas, Campinas, São Paulo, Brazil | [5]University of North Carolina at Chapel Hill, Chapel Hill, North Carolina, USA | [6]Instituto de Biociências, USP, São Paulo, São Paulo, Brazil | [7]Synthetic and System Biology Center, Inova USP, São Paulo, São Paulo, Brazil | [8]Instituto de Biologia, Universidade de Campinas, Campinas, São Paulo, Brazil

Correspondence: Eder M. da Silva (edermarques.silva@gmail.com) | Antonio Figueira (figueira@cena.usp.br)

Received: 10 November 2023 | **Revised:** 28 December 2024 | **Accepted:** 30 December 2024

Funding: This work was supported by Conselho Nacional de Desenvolvimento Científico e Tecnológico and Fundação de Amparo à Pesquisa do Estado de São Paulo.

Keywords: cacao | hormones | lateral roots | sink | witches' broom disease

ABSTRACT

Moniliophthora perniciosa is the causal agent of the witches' broom disease of cacao (*Theobroma cacao*), and it can infect the tomato (*Solanum lycopersicum*) 'Micro-Tom' (MT) cultivar. Typical symptoms of infection are stem swelling and axillary shoot outgrowth, whereas reduction in root biomass is another side effect. Using infected MT, we investigated whether impaired root growth derives from hormonal imbalance or sink competition. Intense stem swelling coincided with a reduction in root biomass, predominantly affecting lateral roots. RNA-seq analyses of root samples identified only a few differentially expressed genes involved in hormone metabolism, and root hormone levels were not expressively altered. Inoculation of the auxin highly-sensitive *entire* mutant genotype maintained the impaired root phenotype; in contrast, the low-cytokinin MT transgenic line overexpressing *CYTOKININ OXIDASE-2* (*35S::AtCKX2*) with fewer symptoms did not exhibit root growth impairment. Genes involved in cell wall, carbohydrate, and amino acid metabolism were down-regulated, accompanied by lower levels of carbohydrate and amino acid in roots, suggesting a reduction in metabolite availability. $^{13}CO_2$ was supplied to MT plants, and less ^{13}C was detected in the roots of infected MT but not in those of *35S::AtCKX2* line plants, suggesting that cytokinin-mediated sugar sink establishment at the infection site may contribute to impaired root growth. Exogenous sucrose application to roots of infected MT plants partially restored root growth. We propose that the impairment of lateral root development is likely attributed to disrupted sugar signalling and photo-assimilate supply by establishing a strong sugar sink at the infected stem.

Summary statement

- We investigated the causes of the impaired root growth of shoot-infected tomato (*Solanum lycopersicum*) Micro-Tom cultivar by *Moniliophthora perniciosa*, the causal agent of the witches' broom disease of cacao.
- We propose that the impairment of lateral root development is likely attributed to disrupted sugar signalling and photoassimilate supply by establishing a strong sugar sink at the infected stem.

1 | Introduction

Plant–pathogen interactions occur either below- or aboveground. Soil-borne pathogens significantly contribute to crop yield losses by directly damaging plant roots (Dutta et al. 2023); however, aboveground colonisers can seldom also impair root development (Nogueira Júnior et al. 2017). Root functions are highly dependent on their plastic and dynamic architecture, commonly shaped by genetic and environmental factors (Rogers and Benfey 2015). Most dicotyledonous plants exhibit root systems with primary and lateral roots (LRs) (Rogers and Benfey 2015). Lateral roots arise from the pericycle founder cells of primary roots (Vermeer et al. 2014), and their recurrent growth shapes the root system (Muller et al. 2019; Reyes-Hernández and Maizel 2023).

Root growth is determined by cell proliferation and elongation, which are regulated by hormones and carbohydrate availability (Stitz et al. 2023). The emergence of LRs depends on long-distance shoot signals (Li, Testerink, and Zhang 2021). Auxin (AUX) is the primary hormone player in root development, and its periodic activation in a concentration dependent-manner dictates meristem activity, with a critical role in the early events of LR development (Marhavý et al. 2013; Motte, Vanneste, and Beeckman 2019). Although AUX signalling from the shoot usually governs LR initiation, emergence, and morphogenesis, auxin-independent pathways have also been reported (Kircher and Schopfer 2023).

Roots rely on shoot-derived sucrose as a primary energy source for growth (Stitz et al. 2023). Additionally, sugars and their derivatives serve as energy sources and signalling molecules (Yu, Lo, and Ho 2015). Photosynthetic sucrose acts as a shoot-to-root signal, inducing periodic LR initiation in an AUX-tuneable manner or root elongation in an AUX-independent pathway (Kircher and Schopfer 2023). Moreover, the central regulator of energy homoeostasis, Target-of-Rapamycin (TOR), modulates the translation of AUX Response Factors (ARF19 and ARF7) and promotes the supply of photosynthetic carbohydrates to the initiation of LR, a process highly dependent on glycolysis (Stitz et al. 2023). Glucose is sensed and transduced through specific glucose sensors or indirectly via TOR and SNF1-RELATED PROTEIN KINASE1 (SnRK1) (Li and Zhao 2024). SnRK1, a key growth regulator under energy-depleted conditions, plays an inhibitory role in LR growth (Crookshanks, Taylor, and Dolan 1998; Morales-Herrera et al. 2023).

Plant pathogens are known to disrupt sugar balance at infection sites to promote susceptibility by inducing invertases (Kocal, Sonnewald, and Sonnewald 2008; Liu et al. 2015). High invertase activity redirects a significant portion of photoassimilates, leading to sugar starvation in other sink regions, including roots (Gorshkov and Tsers 2022). In roots, sugars are absorbed either through symplastic routes or via sugar transporters, such as SUCROSE TRANSPORTER (SUC) and SUGAR WILL BE EXPORTED TRANSPORTER (SWEET), the latter potentially playing a crucial role in mitigating stress conditions (Li, Testerink, and Zhang 2021).

Limited root growth caused by aboveground pathogen infection is often attributed to a compromised supply of photosynthates. Cytokinins (CKs) and AUX are typically involved in plant–pathogen interactions by contributing to the establishment of a strong sink at the infection site, primarily because of their role in promoting cell division and expansion, respectively (McIntyre, Bush, and Argueso 2021). For instance, infection of *Pisum sativum* cotyledons by *Rhodococcus fascians* increased sink strength by the rise in CK and AUX levels and led to reduced root growth (Dhandapani et al. 2017). Infection of *Pistacia atlantica* × *P. integerrima* leaves by *Rhodococcus* led to witches' broom and leafy gall formation and caused twisted roots with limited lateral branching (Stamler et al. 2015; Dhaouadi, Mougou, and Rhouma 2020). Similarly, infection by phytoplasmas that cause witches' broom disease in cassava (by 16SrIII-B subgroup phytoplasma) and Mexican lime (by '*Candidatus* Phytoplasma aurantifolia') was associated with smaller roots, likely because of starch accumulation in the canopy, depriving carbohydrate to the roots (Raiesi and Golmohammadi 2020; Hemmati, Nikooei, and Al-Sadi 2021; Noorizadeh, Khakvar, and Golmohammadi 2022).

Moniliophthora perniciosa is an aboveground pathogen of *Theobroma cacao* (cacao), the causal agent of the witches' broom disease. Basidiospores are the only infective structures targeting meristematic tissues such as the shoot apex, axillary meristems, flowers, and developing fruits (Purdy and Schmidt 1996). After tissue penetration by basidiospore germ tubes, the monokaryotic hyphae grow in the apoplast without specialised feeding structures during the long biotrophic stage of infection. During this stage, prominent shoot symptoms such as loss of apical dominance and abnormal hypertrophic axillary shoots occur. Then, the mycelia go through dikaryotization, invading and killing the host cells, leading to tissue necrosis. *M. perniciosa* can be categorised into biotypes based on host preference: the C-biotype infects *Theobroma* species, the S-biotype infects Solanaceae, including tomato (*Solanum lycopersicum*), and the non-pathogenic L-biotype colonises wild Bignoniaceae lianas (Lisboa et al. 2020).

Since cacao is a perennial tree species, we have adopted the miniature tomato cultivar 'Micro-Tom' (MT) as a model to investigate the molecular and physiological aspects of the interaction with *M. perniciosa* (Deganello et al. 2014). While the reduction in root biomass has been reported as an additional indirect symptom of *M. perniciosa* MT infection (Marelli et al. 2009; Costa et al. 2021), this finding is unprecedented in cacao. Cacao trees exhibit conical taproots with extended LRs, while fine LRs (diameter < 2 cm) grow mainly in the litterfall as the primary driver of water and nutrient uptake (Kummerow, Kummerow, and Souza da Silva 1982; Carmona et al. 2021).

Cacao fine LRs are very plastic, with seasonal periods of turnover associated with leaf flushing and pod production under field conditions, as a result of the redistribution of photosynthates to sustain the reproductive organs (Kummerow, Kummerow, and Souza da Silva 1982; Muñoz and Beer 2001; McCormack et al. 2015).

Previously, we have demonstrated that infection by *M. perniciosa* interferes with the CK and AUX balance in the stems of infected MT plants (Costa et al. 2021). An MT line that overexpresses the Arabidopsis *CYTOKININ OXIDASE-2* gene (*35S::AtCKX2*) (Pino et al. 2022) showed less incidence and symptoms when inoculated (Costa et al. 2021). Infection of MT plants led to the induction of a strong sink at the infected stem but not in the *35S::AtCKX2* MT line (Paschoal et al. 2022). The translocation of sugars and water to the symptomatic region of infection in MT appears to impair host development and fruit yield (Paschoal et al. 2022).

Here, we investigated whether the impairment of LR growth in *M. perniciosa*-infected MT plants was caused by hormonal imbalance or derived from the restriction in photoassimilates by sink competition. Possibly, the cytokinin-mediated sugar sink established at the infection site (stem) (Costa et al. 2021; Paschoal et al. 2022) disrupts sugar signalling and/or restricts the availability of carbon skeleton for proper root development, as indicated by histological, metabolic, and transcriptional rearrangements observed in the roots, and further supported by the reduced ^{13}C content in the roots after pulse-labelling. The growth of LRs in cacao is also impaired by *M. perniciosa* infection, a significant symptom overlooked for decades. We propose that the compromised growth of the root system could hinder water and nutrient uptake in infected MT plants, directly affecting yield, and speculate that similar effects may occur in the roots of cacao plants.

2 | Materials and Methods

2.1 | Plant Material

The plants used in the inoculation experiments were MT, the low CK transgenic line *35S::AtCKX2*, and the mutants *diageotropica* (*dgt*), with low sensitivity to AUX (Oh et al. 2006) and *entire*, with an increased response to AUX (Zhang et al. 2007), all of which are in the MT background (Table 1), along with cacao seedlings. MT and cacao plants were grown as described (Costa et al. 2021). The plants were kept in a growth chamber at 25°C, 14 h photophase, and 80% humidity. For root measurement, MT, *35S::AtCKX2*, *dgt*, and *entire* seeds were germinated in expanded vermiculite, and 7-day-old seedlings were transferred to pots containing Hoagland nutrient solution (Bosse and Köck 1998).

2.2 | Shoot Inoculation

Dry brooms from the Tiradentes isolate (S-biotype) and from the Uruçuca isolate (C-biotype) were obtained from naturally infected stems of *Solanum lycocarpum* and cacao, respectively. Basidiospores were collected as described (Costa et al. 2021). Using a micropipette, the shoot apex and axillary buds of 14-day-old MT and 20-day-old cacao plants were inoculated with 70 μL of 10^6 basidiospores/mL in 0.3% water-agar. Inoculated plants were kept in a humid chamber for 48 h to facilitate infection. Disease symptoms were visually determined, and the tomato stem diameter was measured between the first and second leaves with a digital pachymeter at the indicated periods. The cacao broom was measured at the base with a digital pachymeter. The dry weight of the tomato root and 3-cm stem segment was determined at 20 and 30 d after inoculation (dai); the dry weight of the cacao broom and the root was determined at 20 dai.

2.3 | Anatomical Analyses and Histochemical Staining

Cross-sections of the primary and LRs of inoculated or non-inoculated MT plants were collected and immediately fixed in formalin: acetic acid: 50% ethanol (5:5:90, v/v/v) for 72 h (Johansen 1940). Samples were dehydrated in an ethanol series, washed in propanol and butanol, infiltrated in butanol (3:1, 1:1, 1:3), and embedded in Historesin (Leica; Heidelberg, Germany) for 48 h. Root cross-section (4 μm) was obtained with a Leica RM 2155 rotary microtome (Nussloch, Germany), stained in toluidine blue (Sakai 1973), or Periodic Acid-Schiff (PAS) reagent (Feder and O'Brien 1968). Sections were visualised under an Axioskop 2 upright microscope (Carl Zeiss; Jena, Germany). Root measurements were estimated using ImageJ (https://imagej.nih.gov/ij/). Cross-sections of primary roots were also stained in zinc iodine chloride (Johansen 1940), ferric chloride, or 4% phloroglucinol (Neon; Florianópolis, SC, Brazil) in 37% HCl for 3 min (Jensen et al. 1962). Significant differences

TABLE 1 | Mutants and transgenic-line associated with hormone perception or response introgressed into 'Micro-Tom' (MT) tomato.

	Hormonal class	Description/Phenotype
Mutants		
diageotropica	Auxin	Reduced auxin sensitivity; cyclophilin-defective protein (Oh et al. 2006).
entire	Auxin	Increased auxin sensitivity; *La2922* defective protein, involved in auxin transcription pathway (Zhang et al. 2007).
Transgenic line		
35S::AtCKX2	Cytokinin	Low levels of cytokinin. Overexpression of *AtCKX2* gene (Werner et al. 2003; Pino et al. 2010; Pino et al. 2022).

were determined by the *t*-test at $p < 0.05$ ($n = 3$) using R. Free hand cross-sections of cacao primary roots were obtained from inoculated or noninoculated plants at 30 dai and stained in zinc iodine chloride (Johansen 1940). Sections were visualised under an S8AP0 (Leica) stereomicroscope with apochromatic optics.

2.4 | Lignin Quantification

Roots from inoculated or noninoculated MT plants were collected at 10, 20, and 30 dai, and cacao roots were collected at 30 dai, ground in a cryomill and freeze-dried. Samples were subjected to sequential extraction to prepare cell wall residue (CWR) to estimate total lignin (% cell wall) (Paschoal et al. 2022). Lignin quantification ($n = 4$) was performed using the acetyl bromide method (Fukushima and Kerley 2011).

2.5 | RNA Extraction and RNA-Seq Analysis

Total RNA was extracted using TRIzol (Thermo Fisher Scientific; Waltham, MA, USA). Five biological replicates of roots from inoculated or noninoculated MT plants were collected at 5, 10, 20, and 30 dai. RNA-seq analysis was conducted at the High-Throughput Sequencing Facility at the University of North Carolina, Chapel Hill, NC, USA. Libraries were constructed from mRNA using 1 μg of total RNA using a KAPA Stranded RNA-Seq Kit (Kapa Biosystems; Wilmington, MA, USA). The insert size was approximately 200–300 bp, and dual adapters (2D, TruSeq RNA adapter plate, Illumina; San Diego, CA, USA) were used. Each pool was sequenced in one flow cell lane in single-end 100 bp reads using a HiSeq 4000 sequencer (Illumina). RNA-seq data analysis was conducted as previously described (Costa et al. 2021). A one-way experimental design was adopted to compare five libraries from the roots of inoculated MT plants vs. those of noninoculated plants at each time point using a generalised linear model implemented in edgeR (Robinson, McCarthy, and Smyth 2010). The false discovery rate (FDR) was applied to correct the *p* values after multiple comparisons (Benjamini and Hochberg 1995). Genes with FDR ≤ 0.01 and a fold-change ≥ 2 were considered differentially expressed (DEGs). RNA-seq reads, and the count matrix are available in the NCBI SRA database (PRJNA1032597). Principal component analysis (PCA) was performed using the Abundance Matrix Operations in R (AMOR v. 0.2-2) package (Paredes 2016), based on the 500 genes exhibiting the highest variance across samples. Gene Ontology (GO) term enrichment was analysed using the compareCluster function from the clusterProfiler package in R (Yu et al. 2012). We used MapMan (Thimm et al. 2004) to classify the DEGs into defined hierarchical categories (BINs). Hierarchical clustering analyses were conducted using the ComplexHeatmap package in R (Gu, Eils, and Schlesner 2016), employing the Euclidean distance and complete linkage clustering method.

2.6 | Hormone Quantification

Roots from inoculated or noninoculated MT and cacao plants were used to estimate CKs (isopentenyladenine [iP], dihydrozeatin [DHZ], *trans*-zeatin [tZ]), AUX indole-3-acetic acid (IAA), salicylic acid (SA), jasmonic acid (JA), abscisic acid (ABA) and gibberellic acid (GA_1) levels as previously described (Costa et al. 2021). Roots were collected at 5, 10, 20, and 30 dai ($n = 5$ per time point) for MT or at 30 dai ($n = 5$) for cacao. Hormones were extracted as described by Martínez-Bello, Moritz and López-Díaz (2015) and analysed as described by Costa et al. (2021).

2.7 | Analysis of Primary Metabolites by Gas Chromatography Coupled to Time-of-Flight Mass Spectrometry (GC–TOF–MS)

Roots from inoculated or noninoculated MT plants collected at 5, 10, 20, and 30 dai were ground ($n = 5$ per time point), and metabolites were extracted from 50 mg of samples as described (Giavalisco et al. 2011; Paschoal et al. 2022). The chromatograms were exported from Leco ChromaTOF (v. 4.51.6.0) into cdf files to be processed in R (R Core Team. 2020). TargetSearch (Bioconductor) was used for peak detection and retention-time alignment (Cuadros-Inostroza et al. 2009). The extracted mass spectra and retention times were queried for metabolite identification against the Golm Metabolome database reference library (http://gmd.mpimp-golm.mpg.de/). Metabolites were quantified by the intensity of peaks by quantitative mass. Normalisation of metabolite intensity was achieved by dividing fresh weight and ion counts (Giavalisco et al. 2011), and data were normalised by dividing each value by the average of all measures for one metabolite. Principal component analysis (PCA) was conducted employing pcaMethods in Bioconductor (Stacklies et al. 2007).

2.8 | Root and Total Leaf Area Measurements

Roots of MT, *35S::AtCKX2*, *dgt*, and *entire* plants were collected at 5, 10, and 20 dai, and roots of cacao seedlings were collected at 30 dai, and analysed using WinRHIZO (Regent Instrument; Quebec, Canada). To determine the total root length, volume and area, the roots were placed in a water tray and scanned using an Epson Expression 10 000XL Pro at 800 dpi resolution. Images were analysed using WinRHIZO 2016a (Wang and Zhang 2009). The experimental design was completely randomised in four genotypes × two inoculation conditions factorial for tomato ($n = 6$ per time point). The total leaf area (cm^2) of MT and *35S::AtCKX2* plants was determined using an LI-3100C leaf-area integrator (LI-COR; Lincoln, NE, USA).

2.9 | $^{13}CO_2$ Enrichment

MT and *35S::AtCKX2* plants were grown and inoculated as described earlier. Each acrylic 31L chamber was used to supply $^{13}CO_2$ (Silva et al. 2021) to four contained plants, two MT (inoculated or noninoculated) and two *35S::AtCKX2* plants (inoculated or noninoculated). $^{13}CO_2$ was obtained from a 10 L cylinder containing 99% ^{13}C (Cambridge Isotope Laboratories, Tewksbury, MA, USA). The pot substrate surface was covered by plastic film to avoid a direct supply of $^{13}CO_2$ to the roots. Plants remained inside the chambers for 30 min before the first supply of $^{13}CO_2$. Each chamber received four applications of 20 mL $^{13}CO_2$ at

40-min intervals between 8 and 11 h AM for four consecutive days (Silva et al. 2021). The experimental design was completely randomised ($n = 5$ chambers). Stems and roots were harvested three and 8 days after the last $^{13}CO_2$ enrichment, dried at 60°C, and ground. The samples were subjected to ^{13}C determination using a CH4 Flow Mass Spectrometer (ATLAS MAT; Bremen, Germany). Isotopic analysis is described in File S2.

2.10 | In Vitro Sucrose Supplementation

Tomato seeds were germinated in vitro on semi-solid media (half-strength MS salts, B5 vitamins, 6 g L^{-1} agar) for 1 week when seedlings were transferred to sterilised moist vermiculite in 500-mL jars under sterile conditions. Fifteen days later, 10 mL of 30 mM sucrose was added to the vermiculite. Twenty-day-old plants were then inoculated with *M. perniciosa* basidiospores as described earlier. Two days after inoculation, and subsequently every 10 days, 10 mL of either sterile 10 mM or 60 mM sucrose solution was supplied to the vermiculite substrate. The plants were kept in a growth chamber at 25°C, and 14 h photophase. Root parameters were measured at 35 dai as described earlier.

2.11 | Statistical Analyses

Depending on the specific experiment, statistical differences were determined using the *t*-test, one-way ANOVA, or two-way ANOVA. All data were assessed for the assumptions of parametric analysis. Statistical details are specified in each figure legend.

3 | Results

3.1 | Shoot Infection With *M. perniciosa* Impairs Root Development

MT infection by the S-biotype of *M. perniciosa* reduces root biomass; however, the pathogen could not be detected in the roots (Paschoal et al. 2022). Here, we inoculated MT plants at the shoot apices, and the significant increase in stem diameter at 20 dai (Figure 1a) coincided with the significant reduction in root biomass (Figure 1b,c). To verify whether infection of cacao plants by *M. perniciosa* followed a similar reduction in root growth, we inoculated seedlings at the shoot apex with the C-biotype of *M. perniciosa* (Figure 1d). Infected plants showed an increase in shoot diameter (Figure 1e) and dry weight (Figure S1) together with a decrease in root biomass at 30 dai (Figure 1f).

3.2 | Primary Roots Display Reduced Diameter and Xylem Cross-Section Area and Lower Polysaccharide, Starch, and Phenolic Contents

Cross-sections of regions of the primary roots of inoculated MT plants were analysed by light microscopy (Figure S2). We observed a reduction in the root diameter (Figure 2a,d,e) and xylem area (Figure 2b,f,g) of inoculated plants in comparison to noninoculated controls; no difference was observed for the phloem area (Figure 2c). After specific staining, lower polysaccharide (Figure 2h,i), starch (Figure S3a), and phenolic (Figure S3b) contents were observed in the roots of inoculated MT plants. However, no changes in lignin content were evidenced by phloroglucinol-HCl staining (Figure S3c). Accordingly, the levels of lignin were not significantly different between roots from inoculated and noninoculated MT plants (Figure S3d).

Likewise, no significant difference in lignin content was observed between the roots of inoculated and noninoculated cacao seedlings (Figure S3e). Cross-sections of primary roots from inoculated cacao seedlings showed reduced starch content, along with visible thinning and reduced xylem, consistent with the results observed in MT (Figure S4a–c).

We also analysed cross-sections of LRs of MT tomato emerging from the region of the primary roots used for histology (Figure S2). LRs did not differ in diameter (Figure S5a). Nevertheless, histology after blue toluidine staining revealed lower polysaccharide contents in the LRs of inoculated MT plants (Figure S5b,c).

3.3 | Hormones Appear to Play a Minor Role in the Impairment of Root Growth

A time-course RNA-seq analysis of roots from inoculated MT plants was conducted to identify presumed causes for root growth impairment. While most of the variation in the root transcriptional profile was related to the time of sampling (5, 10, 20, or 30 dai), roots from inoculated MT plants exhibited a distinct transcript profile from noninoculated controls as early as 20 dai (Figure S6a), when impaired root growth was first observed (Figure 1b). Hundreds of differentially expressed genes (DEGs) were detected in inoculated plants at all-time points, with the highest number of DEGs observed at 30 dai (Figure S6b). From 20 dai, upregulated genes were associated with AUX response, response to toxic compounds, and transmembrane transport of water and anion (Figure S6c). By 30 dai, genes related to cell organisation, root hair development, and nitrate response were enriched (Figure S6c). Downregulated genes were linked to responses to water, light, oxidative stress, and ABA signalling at 30 dai (Figure S6c).

To specifically investigate hormonal metabolism by changes in the transcriptional profile, members of well-known gene families related to hormone metabolism were compared between samples of roots of inoculated or noninoculated plants at each time point (Figure 3a). The annotation within each group is shown in File S1; DEGs are presented in Table S2. Overall, genes related to ABA, ethylene (ET), and CK metabolism were downregulated. Genes involved in ABA signalling and oxidation were repressed, except for one gene encoding the ABA receptor PYL4-like and another encoding a cytochrome P450 with ABA 8′-hydroxylase activity, both of which were induced (Figure 3a Table S1). Genes involved in ET biosynthesis (ACC oxidase), perception and signal transduction (*Never-ripe 2*), and CK biosynthesis (adenylate isopentenyl transferase and CK riboside 5′-monophosphate phosphoribohydrolase), as well as CK transport (ABC transporter-like), response (two-component response regulator), and oxidation (CK oxidase/dehydrogenase), were consistently downregulated (Figure 3a).

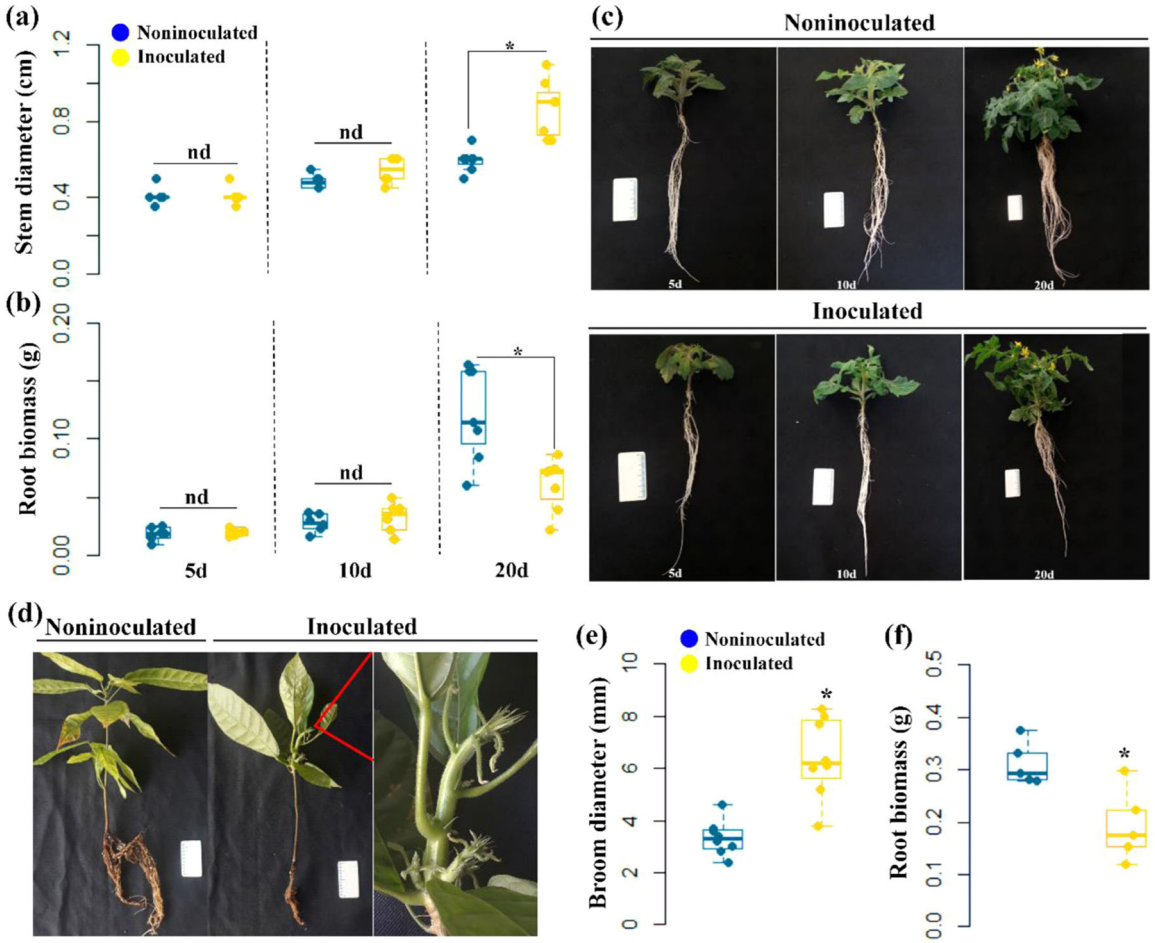

FIGURE 1 | Infection of 'Micro-Tom' (MT) tomato (*Solanum lycopersicum*) and cacao (*Theobroma cacao*) plants inoculated at the shoot apex and axillary buds with isolates of the S-biotype or the C-biotype of *Moniliophthora perniciosa*, respectively, reduces root biomass. (a) Stem diameter and (b) root dry weight of noninoculated or inoculated MT plants with the S-biotype of *M. perniciosa* at 5, 10, or 20 days after inoculation (dai) ($n = 6$). (c) Representative pictures comparing noninoculated (upper panel) or inoculated (lower panel) MT plants at 5 (at left), 10 (at the middle), and 20 (at right) dai. (d) Representative pictures comparing noninoculated (at left) or inoculated (at right) cacao plants with the C-biotype of *M. perniciosa* at 20 dai. Red lines indicate picture inset of stem-thickening symptoms. (e) Stem diameter of noninoculated or inoculated ('broom') cacao plants at 20 dai ($n = 8$). (f) Root dry weight of noninoculated or inoculated cacao plants at 20 dai ($n = 5$). Statistically significant differences were determined by the *t*-test at 5% probability. In each boxplot, the middle line represents the median value, the upper and lower bars correspond to the first and third quartiles, respectively, and the whiskers represent 1.5 times the interquartile range.

While the AUX repressor AUX-regulated IAA15 and a PIL-like efflux carrier were repressed, the genes encoding the members of AUX biosynthesis indole-3-acetic acid-amido synthetase were induced at 30 dai (Figure 3a).

We also quantified the levels of gibberellin (GA_1), JA, ABA, iP, DHZ, tZ, IAA, and SA in roots at 20 dai, when we first observed a reduction in root biomass, and later at 30 dai (Figure 3b–i). The levels of JA increased at 20 dai compared with the noninoculated control (Figure 3g), while the levels of GA_1, ABA, and SA were not significantly different between treatments (Figure 3a,d,i). Regarding CKs, only DHZ levels exhibited a significant reduction at 20 dai (Figure 3e), corroborating the cytokinin transcriptional behaviour; iP and tZ levels did not display significant differences at 20 or 30 dai comparing inoculated with the noninoculated control (Figure 3f,g). Despite the repression of a few genes associated with AUX response and increase in the expression of one auxin biosynthetic gene, we did not observe significant changes in root IAA levels of inoculated plants (Figure 3h).

To verify whether the hormonal profile of cacao roots after inoculation with the C-biotype of *M. perniciosa* displayed a similar pattern as MT roots, we quantified the same hormones at 30 dai, but none of the analysed hormones presented any significant difference from noninoculated controls (Figure S7).

To functionally investigate whether the CK and AUX imbalance at the infected stem (Costa et al. 2021) could impact root development, we inoculated two AUX mutants, *dgt* and *entire*, plus the transgenic line *35S::AtCKX2*, all in the MT genetic background (Figure S8). The stem diameter of MT, *dgt*, and *entire*, but not *35S::AtCKX2*, increased at 20 dai (Figure 4a). Inoculated MT and *entire* plants exhibited reduced root dry weight compared with noninoculated controls, but not *dgt* and *35S::AtCKX2* plants (Figure 4b). Since AUX is associated with the promotion of LR development, we expected that inoculation of the *entire* genotype would recover the impaired root phenotype; however, this was not the case.

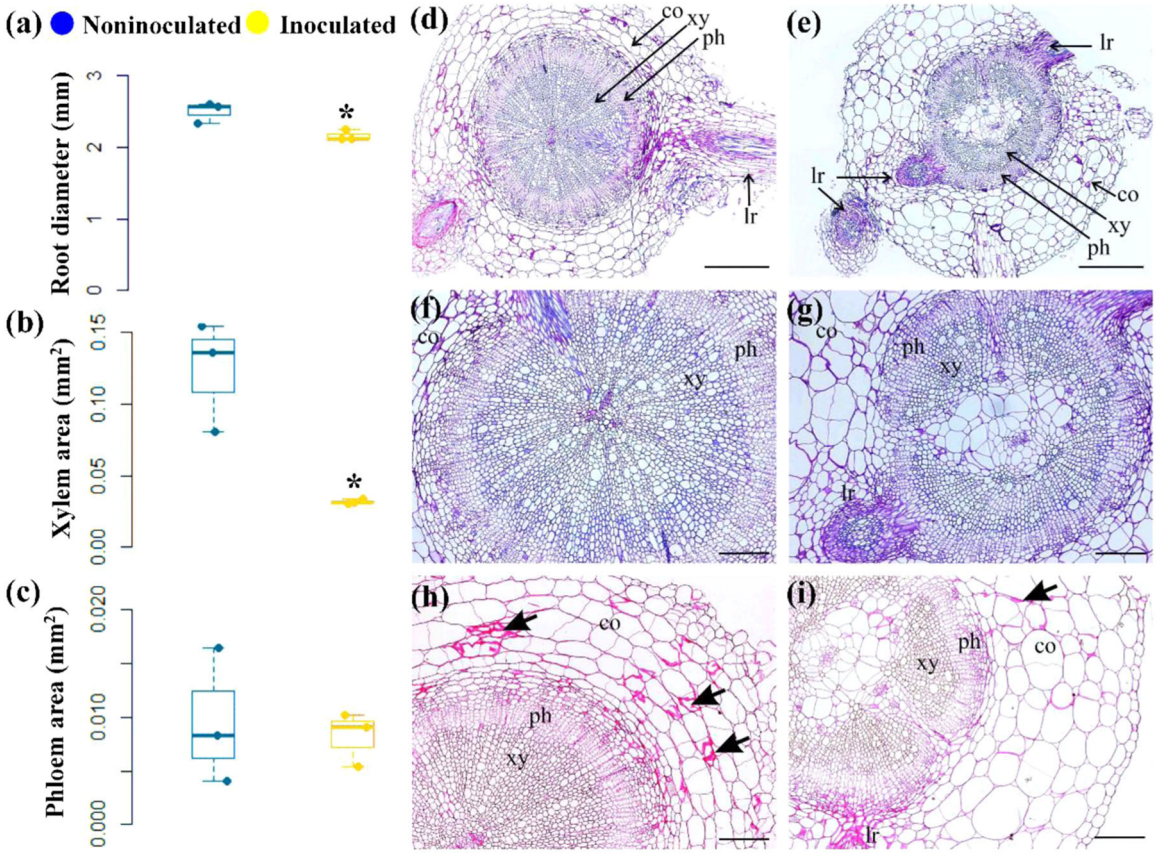

FIGURE 2 | Infection of 'Micro-Tom' (MT) tomato (*Solanum lycopersicum*) with the S-biotype of *Moniliophthora perniciosa* reduces primary root diameter and xylem area. (a) Primary root diameter of noninoculated or inoculated MT plants with *M. perniciosa* at 20 days after inoculation (dai) (n = mean of 10 cross-sections of three biological replicates). (b) Xylem and (c) phloem cross-section area of the primary root of noninoculated or inoculated MT plants at 20 dai. (n = mean of 10 cross-sections of three biological replicates). Statistically significant differences were determined by the t-test at 5% probability indicated by *. In each boxplot, the middle line represents the median value, the upper and lower bars correspond to the first and third quartiles, respectively, and the whiskers represent 1.5 times the interquartile range. Histology of primary root cross-sections of (d), (f) noninoculated or (e), (g) inoculated MT plants stained with blue toluidine. Histology of primary root cross-sections of (h) noninoculated or (i) inoculated MT plants stained with periodic acid-Schiff ($n = 3$). co, cortex; lr, emerging lateral root; ph, phloem; xy, xylem; bold arrows indicate polysaccharide contents. Bars: (d and e) = 500 μm; (f–i) = 200 μm. [Color figure can be viewed at wileyonlinelibrary.com]

3.4 | Shoot Infection Mainly Affects LRs

To identify which parts of the root system of MT, *35S::AtCKX2, dgt*, *entire* are mostly affected by infection with *M. perniciosa*, we estimated root size using image scanning by WinRHIZO. We observed a decrease in total root volume (Figure 4c) and projected area (Figure 4d) in inoculated MT and *entire* genotypes compared with noninoculated controls. Specifically, MT and *entire* infection caused a reduction in total LR length, considering roots from 0 to 0.5 mm long (Figure 4e) and from 0.5 to 1 mm long (Figure 4f). Despite the stem thickening of inoculated *dgt*, this genotype with fewer LRs did not show changes in root biomass, volume or LR length. Therefore, infection with *M. perniciosa* appears to impair LR growth.

To evaluate whether the pattern of impaired LR growth also occurs in cacao, we evaluated roots from cacao seedlings infected with the C-biotype of *M. perniciosa*. Inoculated cacao displayed a reduction in root volume and total LR length considering roots from 2.5 to 3 mm long (Figure S9a,b) and from 4 to 4.5 mm long (Figure S9c,d), demonstrating that LRs are similarly affected in cacao.

3.5 | Roots Undergo Transcriptional Changes Related to Cell Wall Modification

RNA-seq analysis identified DEGs associated with cell wall modification in the roots of inoculated MT plants (Table S1; Table S2). Genes related to hemicellulose biosynthesis were predominantly upregulated. In contrast, those involved in cutin, suberin, and pectin biosynthesis—including a β-xylosidase, a β-galactosidase, and a lipid transfer protein—were downregulated at 20 dai. Additional genes encoding proteins such as glycoside hydrolases, hexosyltransferases, fatty acid hydroxylase, xylosidases, pectin-acetyl esterases, and lipid transfer were repressed at 30 dai (Figure 5a).

Analyses of primary metabolites from roots of inoculated MT plants compared with noninoculated controls (Table S3) detected by GC-TOF-MS showed variability mainly based on the time of sampling (5, 10, 20, or 30 dai). However, inoculated and noninoculated samples became distinctly separated from 20 to 30 dai (Figure S10). A significant change in the relative accumulation of 35 metabolites was observed in the roots (Figure 5b,

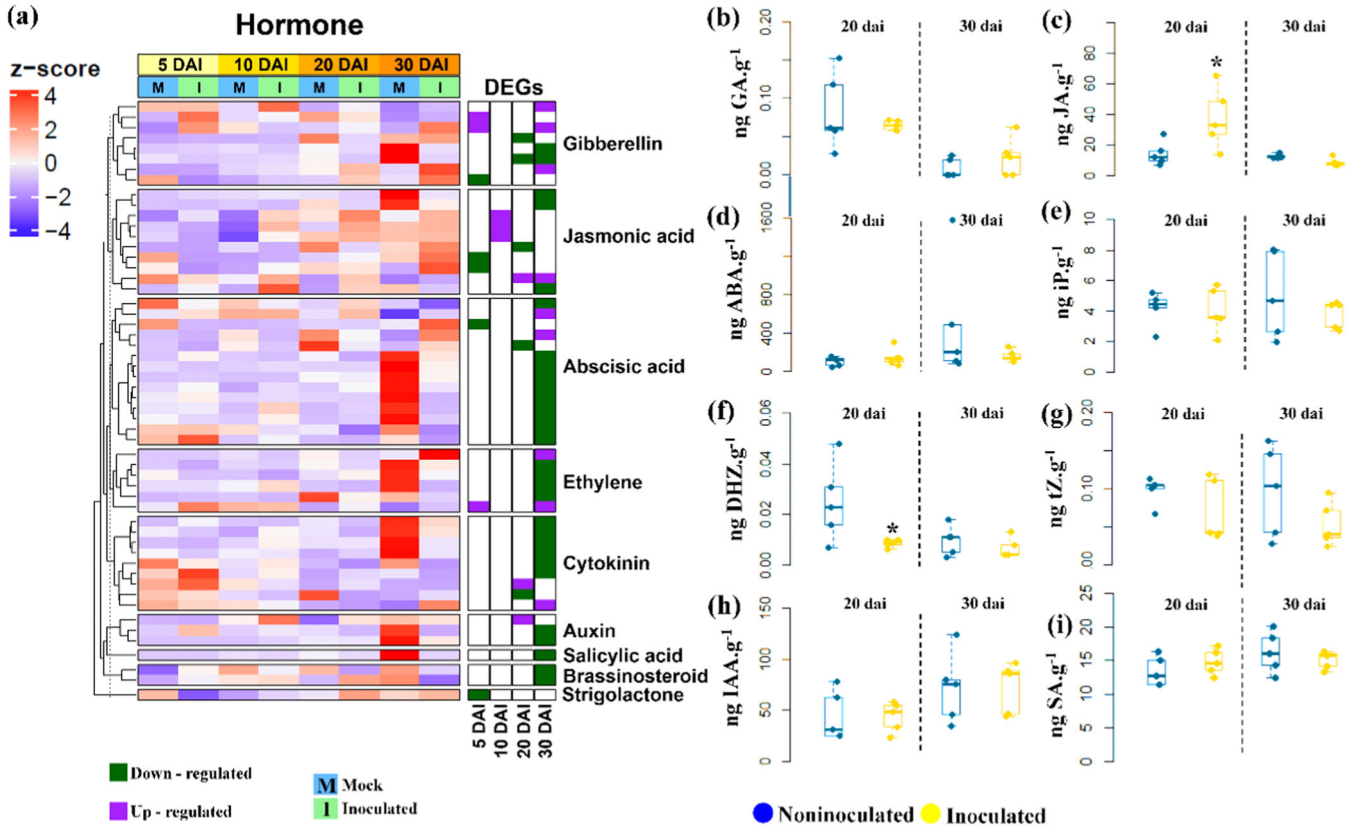

FIGURE 3 | Transcriptomic and hormonal profiling of the roots of inoculated 'Micro-Tom' (MT) tomato (*Solanum lycopersicum*) plants with the S-biotype of *Moniliophthora perniciosa*. (a) Heatmap of differentially expressed genes (DEGs) associated with hormones in the roots of inoculated compared to noninoculated MT plants at 5, 10, 20, or 30 days after inoculation (dai) obtained via RNA-seq analysis ($n = 5$). Scale bar represents values in *z*-score TPM. Genes with $\log_2$ (FC) ≥ 2 or ≤ -2; FDR ≤ 0.01 were considered differentially expressed when comparing inoculated to mock plants. Upregulated DEGs were marked in purple; downregulated DEGs were marked in green. M represents mock (noninoculated); I represents inoculated plants with the S-biotype of *M. perniciosa*. MapMan (Thimm et al. 2004) was used to classify the DEGs into defined hierarchical categories (BINs). Quantification of (b) indole-3-acetic acid (IAA), (c) isopentenyladenine (iP), (d) dihydrozeatin (DHZ), (e) *trans*-zeatin (tZ), (f) gibberellic acid (GA_1), (g) jasmonic acid (JA), (h) salicylic acid (SA), and (i) abscisic acid (ABA) in roots from noninoculated and inoculated MT plants at 20 or 30 dai ($n = 5$). Statistically significant differences were determined by the *t*-test at 5% probability, comparing inoculated with noninoculated plants at the same time point. In each boxplot, the middle line represents the median value, the upper and lower bars correspond to the first and third quartiles, respectively, and the whiskers represent 1.5 times the interquartile range. [Color figure can be viewed at wileyonlinelibrary.com]

Table S3, Figure S11), with notable metabolic reprogramming at 20 dai. Metabolites associated with cell wall modification, such as galactonate, glucarate, and glycerol, accumulated at 20 dai (Figure 5b). Levels of chlorogenic acid, possibly involved in root development or lignin biosynthesis (Franklin and Dias 2011; Silva, Mazzafera, and Cesarino 2019), were reduced at 20 dai but increased again at 30 dai (Figure 5b).

3.6 | Roots Undergo an Adjustment of Energy/Carbon Sources Upon Shoot Infection

To determine whether changes in sugar metabolism drive changes in root development, we investigated the expression of genes related to carbohydrate metabolism and measured carbohydrate levels. Genes involved in oligosaccharide metabolism, such as α-galactosidase, hexosyltransferase, and α-galactosidase, as well as those related to sucrose and starch metabolism, including ADP-glucose pyrophosphorylase, sucrose synthase and hexokinase-6 (a key enzyme in the glucose metabolism via glycolysis) (Figure 6a, Table S1) were consistently downregulated. Sugar transporters, including the monosaccharide transporter SlSFP7, Sugar Transporter Protein 2, Sugar Facilitator Protein 1, bidirectional sugar transporter SWEET (putatively orthologous to Arabidopsis AtSWEET11/12/13/14), PLASTID GLUCOSE TRANSLOCATOR 2 (pGlcT), and SlSUT1, along with genes involved in TOR signalling and regulation of SnRK1 were downregulated at 30 dai (Table S1). In contrast, genes associated with cellular fermentation processes and trehalose metabolism were upregulated at 30 dai (Figure 6a).

In line with the downregulation of genes involved in carbohydrate metabolism, levels of glucose and fructose decreased starting at 10 dai and continued to decline at 20 dai (Figures 6b, and S11), potentially leading to reduced root biomass. The relative increase in trehalose levels (Figures 6b, and S11) corroborates the transcriptomic data (Figure 6a), suggesting that roots may be undergoing stress-induced cellular survival mechanisms. Overall, the data indicate a nutrient, energy, and carbon deficiency in the roots, which could adversely affect root growth.

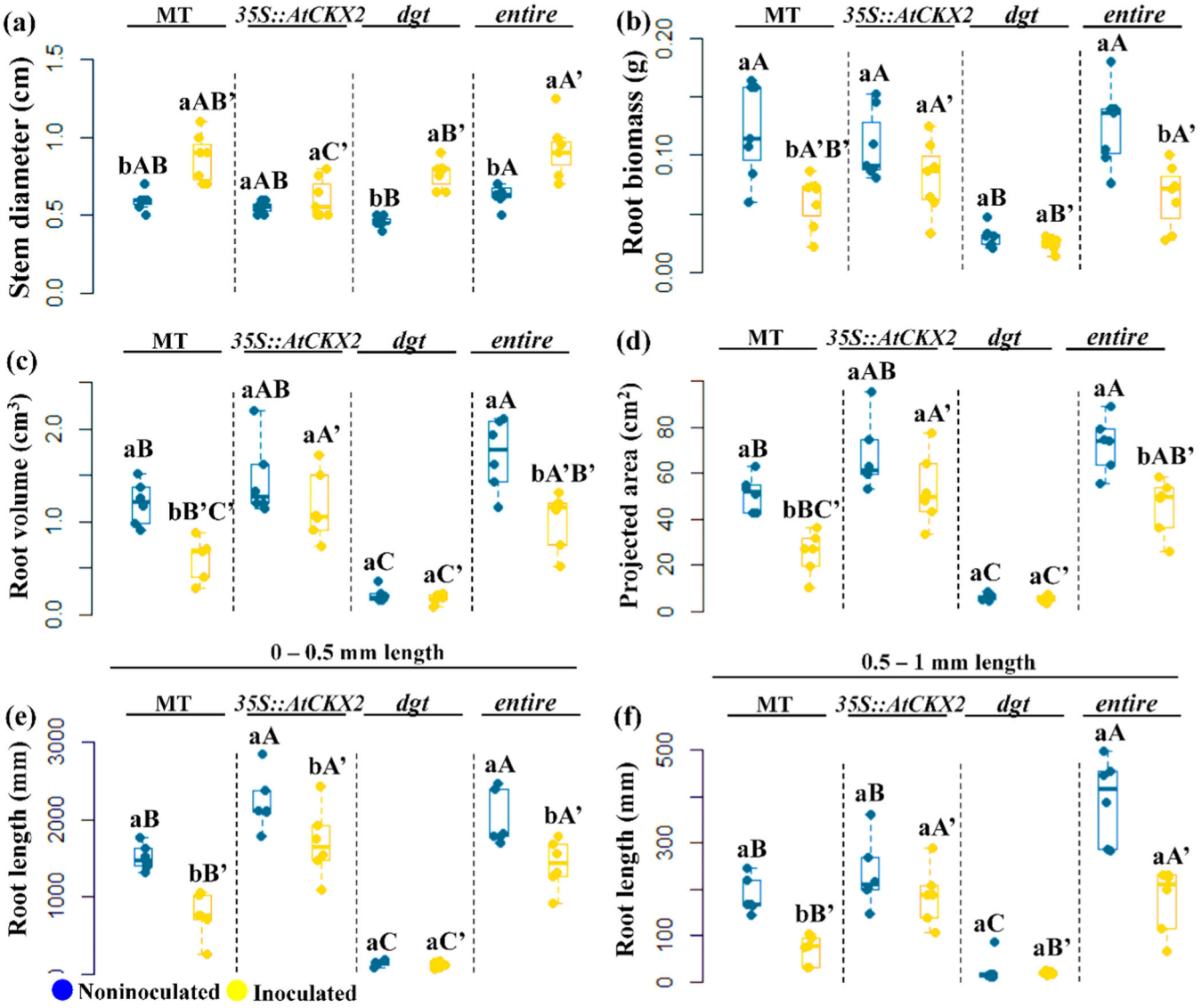

FIGURE 4 | Biometric evaluation of roots in transgenic lines and hormonal mutants (metabolism or perception) in the 'Micro-Tom' (MT) tomato (*Solanum lycopersicum*) background in response to inoculation with the S-biotype of *Moniliophthora perniciosa*. (a) Stem diameter, (b) total root biomass (dry weight), (c) total root volume, (d) total root projected area, (e) total length of roots 0 to 0.5 mm long, (f) total length of roots 0.5 to 1 mm long from MT, *35S::AtCKX2*, *diageotropica* (*dgt*), and *entire* noninoculated or inoculated plants at 20 days after inoculation (dai) ($n = 6$). Statistically significant differences were determined by two-way ANOVA, followed by the Tukey test at 5% probability. Different lowercase letters indicate significant differences between inoculated or noninoculated plants within each genotype; different uppercase letters indicate significant differences among the noninoculated genotypes; different uppercase letters with ' indicate significant differences among the inoculated genotypes. In each boxplot, the middle line represents the median value, the upper and lower bars correspond to the first and third quartiles, respectively, and the whiskers represent 1.5 times the interquartile range. [Color figure can be viewed at wileyonlinelibrary.com]

3.7 | Roots of MT, but Not of *35S::AtCKX2*, Accumulate Less ^{13}C

Inoculation of *35S::AtCKX2* plants resulted in less severe shoot symptoms compared with MT (Figure 4a) and did not significantly impair root development (Figure 4b). Therefore, we hypothesised that root impairment might be associated with the formation of a strong sink at the site of infection, limiting the availability of photosynthates to the roots. Infected *35S::AtCKX2* plants did not display a reduction in plant height (Figure S12a) or in total leaf area (Figure S12b), suggesting that the physiological constraints observed in MT plants by sink establishment (Paschoal et al. 2022) are not observed in *35S::AtCKX2* plants.

We exposed infected MT and *35S::AtCKX2* plants to $^{13}CO_2$ for two h d^{-1} for four d (Figure S13). Compared with non-inoculated plants, inoculated MT plants displayed relatively less ^{13}C accumulation in the roots at 3 days after exposure (dae) and at eight dae, corresponding to 15 or 25 dai, respectively (Figure 6c). Conversely, no difference was observed when comparing roots of inoculated *35S::AtCKX2* with the non-inoculated control (Figure 6d), suggesting that *35S::AtCKX2*, which does not form a sink at the infection site, does not limit root growth and exhibits no difference in ^{13}C in the roots.

In addition, in vitro supplementation of sucrose in a vermiculite substrate partially restored the total root volume (Figure 6d)

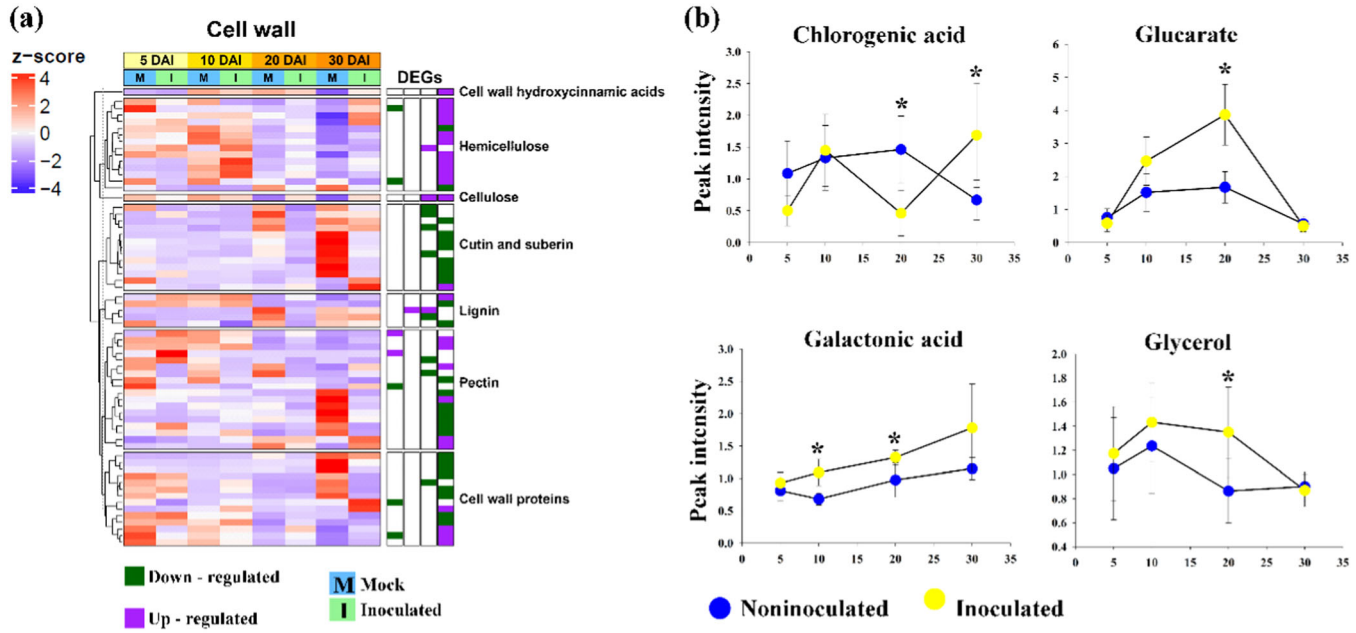

FIGURE 5 | Gene expression and metabolite changes associated with cell wall metabolism of roots of 'Micro-Tom' (MT) tomato (*Solanum lycopersicum*) plants after inoculation with the S-biotype of *Moniliophthora perniciosa*. (a) Heatmap of differentially expressed genes (DEGs) associated with cell wall metabolism in roots from inoculated compared to noninoculated MT plants at 5, 10, 20, or 30 days after inoculation (dai) ($n = 5$), obtained via RNA-seq analysis. Scale bar represents values in z-score TPM. Genes with $\log_2$ (FC) ≥ 2 or ≤ -2; FDR ≤ 0.01 were considered differentially expressed when comparing inoculated to mock plants. Upregulated DEGs were marked in purple; downregulated DEGs were marked in green. M represents mock (noninoculated) and I represents inoculated plants with the S-biotype of *M. perniciosa*. MapMan (Thimm et al. 2004) was used to classify DEGs into defined hierarchical categories (BINs). (b) Mean peak intensity normalised by total ion count and sample mass ±SE of metabolites (Chlorogenic acid, Glucarate, Galactonic acid, Glycerol) hypothetically involved in cell wall metabolism with significant changes in roots from noninoculated or inoculated plants at 5, 10, 20 or 30 dai, identified by gas chromatography coupled to time-of-flight mass spectrometry (GC–TOF–MS; $n = 6$). Statistically significant differences were determined by t-test at 5% probability, comparing inoculated and noninoculated control plants at the same time point, indicated by *. SE = standard error. [Color figure can be viewed at wileyonlinelibrary.com]

and lateral root growth of infected plants, particularly for roots measuring 0.5 to 1 mm long (Figure 6e) and 1.5 to 2 mm long (Figure 6f). In comparison, noninoculated plants exhibited increased lateral root length in response to sucrose supplementation (Figure 6e–f), which has been proposed to be a better carbon source for the development of tomato roots (Devaux et al. 2003; González-Hernández et al. 2020).

3.8 | Shoot Infection Impacts Glycolysis, the Tricarboxylic Acid (TCA) Cycle, and Amino Acid Metabolism in Roots

The transcriptional data suggest that reduced glucose availability in the roots may have impaired the glycolysis pathway, as evidenced by the downregulation of genes encoding key enzymes such as Hexokinase-6 (HXK6) and ATP-dependent 6-phosphofructokinase (PFK) at 30 and 20 dai, respectively (Figure 7, Tables S1, S2). Notably, levels of several amino acids, including valine, alanine, serine, leucine, threonine, proline, and 4-aminobutyrate (GABA), showed significant reduction at 20 dai, coinciding with the onset of impaired root growth (Figure 7). Moreover, several genes related to amino acid metabolism and transport (Figure S14, Tables S1, and S2) were downregulated in the roots of inoculated plants at 30 dai. Conversely, a set of genes involved in cationic amino acid transporters, glutamate decarboxylases, and branched-chain aminotransferase (*SlBCAT6*), potentially involved in the recycling of branched-chain amino acids (Maloney et al. 2010), and *3-HYDROXYISOBUTYRYL-COA HYDROLASE*, associated with amino acid catabolism, were induced at 20 and 30 dai (Figure S14). These transcriptional changes corroborate the observed reduction in amino acid levels in the impaired roots.

The decline in amino acid levels could be attributed to the reduced glycolytic activity or the oxidation of these amino acids to supply energy via their incorporation into the TCA cycle. The accumulation of TCA cycle intermediates, such as malate, fumarate, and citrate, supports this hypothesis (Figure 7; Table S3). Accordingly, genes involved in cellular respiration and coenzyme metabolism showed significant repression at 30 dai, including those encoding nudix hydrolase, cytochrome-c oxidase, and external alternative NAD(P)H-ubiquinone oxidoreductase, which are critical components of oxidative phosphorylation and energy metabolism (Table S1). These findings align with the observed low energetic status of the roots.

3.9 | Roots Undergo Transcriptional Changes Indicative of Abiotic Stress and Nutritional Deficiencies

Genes categorised as related to abiotic stresses were upregulated in the roots of infected MT plants, including several

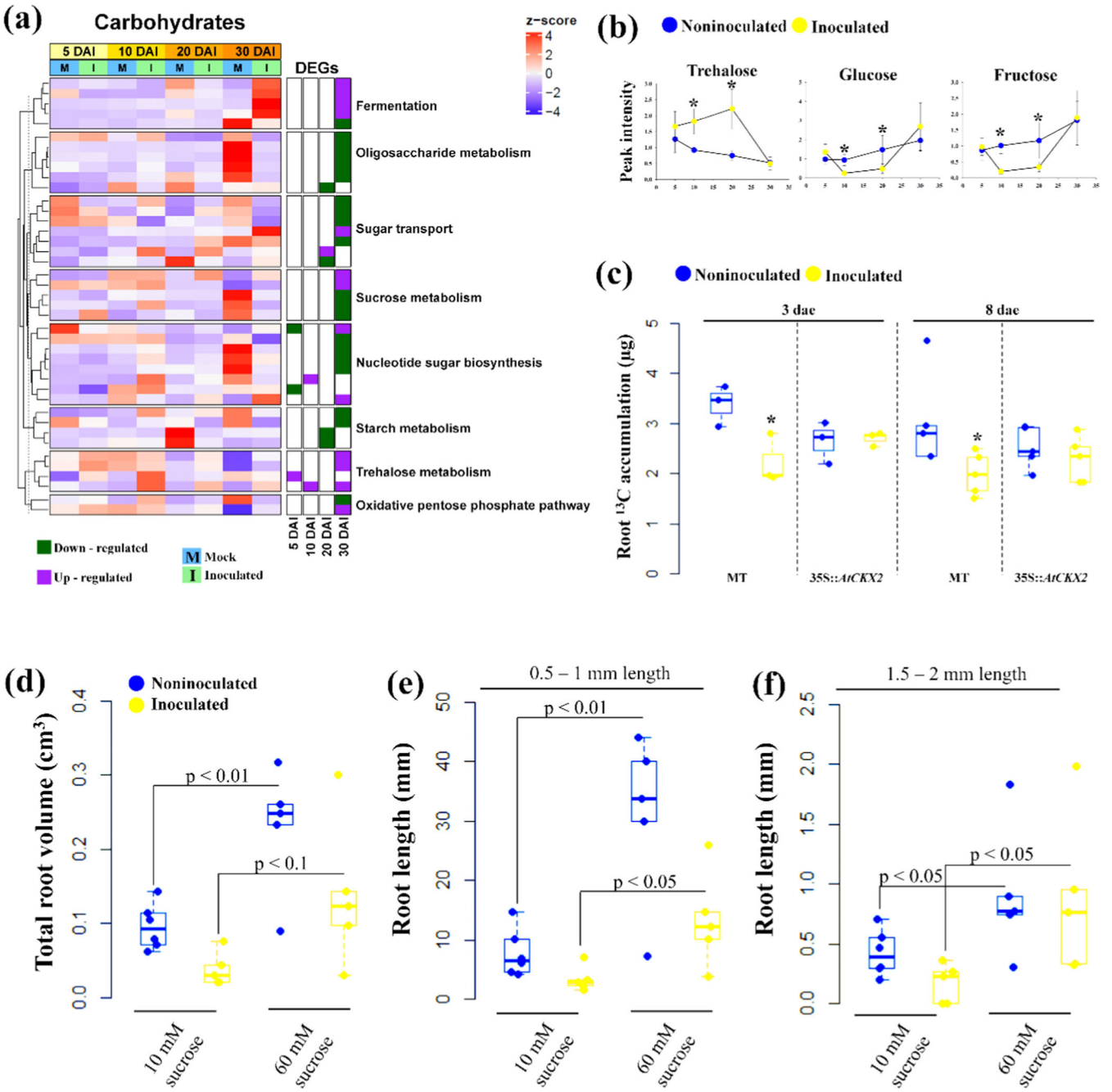

FIGURE 6 | Gene expression and metabolite changes associated with carbohydrate metabolism of roots of 'Micro-Tom' (MT) tomato (*Solanum lycopersicum*) plants after inoculation with the S-biotype of *Moniliophthora perniciosa*. (a) Heatmap of differentially expressed genes (DEGs) associated with carbohydrate metabolism in roots from inoculated compared to noninoculated MT plants at 5, 10, 20, or days after inoculation (dai), obtained via RNA-seq analysis ($n = 5$). Scale bar represents values in z-score TPM. Genes with $\log_2$ (FC) ≥ 2 or ≤ -2; FDR ≤ 0.01 were considered differentially expressed when comparing inoculated to mock plants. Upregulated DEGs were marked in purple; downregulated DEGs were marked in green. M represents mock (noninoculated) and I represents inoculated plants with the S-biotype of *M. perniciosa*. MapMan (Thimm et al. 2004) was used to classify DEGs into defined hierarchical categories (BINs). (b) Mean peak intensity normalised by total ion count and sample mass ±SE of sugars (Trehalose, Glucose, Fructose) with significant changes in roots from noninoculated or inoculated plants at 5, 10, 20 or 30 dai identified by GC–TOF–MS ($n = 6$). (c) ^{13}C accumulation in 0.2 mg samples of roots of MT or *35S::AtCKX2* plants after exposure of shoots to $^{13}CO_2$ after 3 or 8 days ($n = 5$; File S1). Statistically significant differences were determined by the t-test at 5% probability, comparing inoculated and noninoculated plants within the same genotype, indicated by *. (d) total root volume, (e) total length of roots 0.5 to 1 mm long, (f) total length of roots 1.5 to 2 mm long of MT plants inoculated or not, supplied with 10 mM or 60 mM of sucrose. Statistically significant differences were determined by the t-test, comparing plants supplied with 10 and 60 mM sucrose, with significance indicated by the p value. In each boxplot, the middle line represents the median value, the upper and lower bars correspond to the first and third quartiles, respectively, and the whiskers represent 1.5 times the interquartile range. [Color figure can be viewed at wileyonlinelibrary.com]

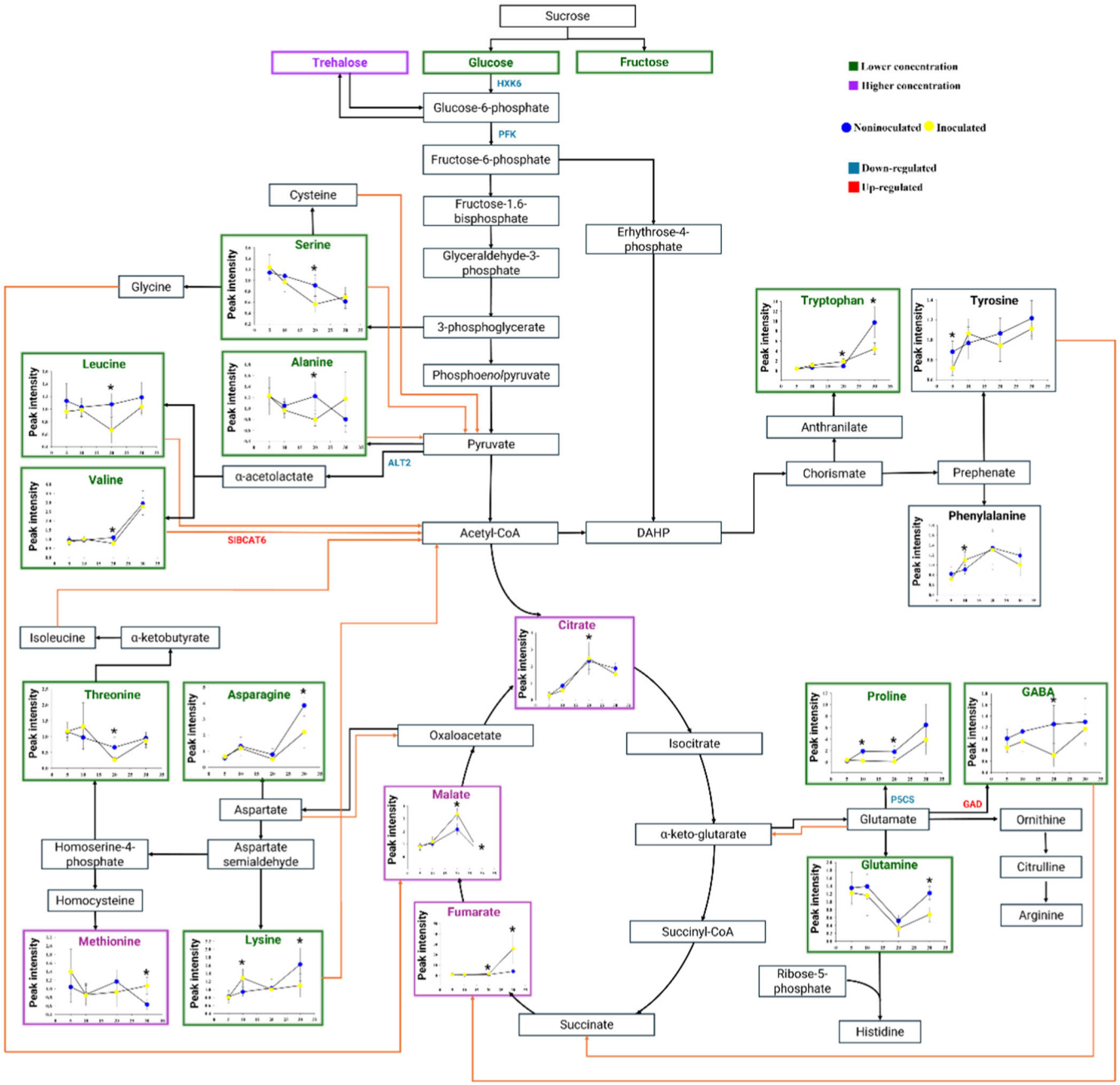

FIGURE 7 | Metabolic rearrangement of roots of 'Micro-Tom' (MT) tomato (*Solanum lycopersicum*) plants after inoculation with the S-biotype of *Moniliophthora perniciosa*. A schematic representation of glycolysis, the tricarboxylic acid (TCA) cycle, and amino acid biosynthetic and catabolic pathways illustrates changes in metabolite levels and the expression of genes encoding key enzymes in these pathways. Line graphs of metabolite levels show mean peak intensity, normalised by total ion count and sample mass ±SE, with significant differences between inoculated and noninoculated roots at 5, 10, 20, or 30 days after inoculation (dai), identified by GC–TOF–MS ($n = 6$). Statistically significant differences were determined by the *t*-test at 5% probability, indicated by an asterisk (*), comparing inoculated and noninoculated plants at the same time point. SE represents standard error. Green outlines around the line graphs indicate lower metabolite levels in inoculated plants, while purple outlines indicate metabolite accumulation in inoculated plants at 20 dai. Gene expression levels are shown in blue for downregulated differentially expressed genes (DEGs) and red for upregulated DEGs in inoculated plants. Genes with $\log_2$ (FC) ≥ 2 or ≤ −2; FDR ≤ 0.01 were considered differentially expressed when comparing inoculated to mock plants. Detailed gene expression data is provided in Tables S1 and S2. [Color figure can be viewed at wileyonlinelibrary.com]

tonoplast intrinsic proteins and aquaporins, which are potentially linked to water stress response (Table S1). This fact, combined with the observed increase in trehalose and raffinose metabolism (Figures 6, 7; and S11) and the reduction in amino acids and carbohydrate levels (Figures 6b and 7, Figure S11), suggests that the roots of infected plants are experiencing stress.

Additionally, several genes involved in nitrogen metabolism, such as high-affinity nitrogen transporters and nitrogen

reductases, were upregulated in the roots of infected plants at 20 and/or 30 dai (Figure S15). By 30 dai, further reduction in glutamine, lysine, and asparagine levels and increased methionine levels (Figures 7, and S11), suggest an impact on nitrogen metabolism. A set of genes that include low-affinity nitrate transporters was repressed either at 20 and/or 30 dai (Figure S15). Likewise, the metabolism of phosphate is transcriptionally activated with the induction of phosphate transporter genes at 20 and/or 30 dai (Figure S15), commonly upregulated under phosphate starvation (Castrillo et al. 2017), along with a decrease in phosphate levels in the roots of infected plants at 30 dai (Figure S11, Table S3).

4 | Discussion

Studies have associated LR growth with crop yield (Duque and Villordon 2019; Zhang et al. 2023). Particularly in cacao trees, fine root steady-state has been associated with water and nutrient uptake, contributing to yield, nutrient recycling, and carbon sequestration (Almeida and Valle 2010). The establishment of witches' broom disease in cacao stands leads to chronic yield losses. Still, the presumed indirect impact of infection in the root system is a nonobvious symptom that remains unexplored. Here, we demonstrated that cacao seedling roots are impaired upon infection by *M. perniciosa*; however, estimating root parameters in cacao trees is challenging.

The availability of the MT model allowed the evaluation of mechanisms involved in root growth impairment. The reduced root size of tomato plants after *M. perniciosa* infection was previously reported (Marelli et al. 2009; Costa et al. 2021); however, the specific factors underlying impaired root growth remained unknown (Paschoal et al. 2022). Here, we showed that the metabolic rearrangement of MT roots and the limited availability and/or signalling of carbohydrates might affect root growth after infection.

We have shown that the major symptom of *M. perniciosa* infection of MT is stem swelling and xylogenesis mediated by CKs (Costa et al. 2021), inducing a sink of carbon skeleton and other nutrients that likely leads to a decrease in net photosynthesis, reducing total flower and fruit production (Paschoal et al. 2022). Here, symptom evaluation of stems (infection site) and roots (distal region) after *M. perniciosa* infection of MT showed a concurrent reduction in root biomass with stem enlargement. Since *M. perniciosa* was not detected in root tissue after inoculation (Paschoal et al. 2022), root symptoms are likely an indirect effect of infection.

After infection of MT or cacao plants, the total LR length of particular length categories was reduced, accounting for total root length and biomass reduction. Although AUX is the primary hormone related to LR development, we could not associate the decrease in total LR length with less AUX or repression of auxin-related genes in MT roots. Inoculation of the *entire* plants indicated that their increased response to AUX was not sufficient to prevent the reduction or recovery of LR growth. However, because we analysed IAA levels and related transcripts in the whole root system, the spatial-specific auxin concentration/gradient was not evaluated. Indeed, the auxin-mediated regulation of LR emergence/elongation is a refined time-space-specific mechanism dependent on an oscillating auxin gradient and gene expression (Perianez-Rodriguez et al. 2021; Torres-Martínez, Napsucialy-Mendivil, and Dubrovsky 2022).

When symptoms became prominent, we observed the downregulation of several genes associated with carbohydrate metabolism and low levels of sugars in MT roots. In particular, we identified the repression of a bidirectional sugar transporter *SWEET* gene orthologous to *AtSWEET11/12/13/14*, which is involved in sucrose transport/phloem loading (Chen et al. 2012), suggesting a restriction of carbohydrate loading into roots of infected plants. The downregulation of *SWEET11* has been associated with a reduction in Arabidopsis root growth (Wang et al. 2023). The repression of other sugar transporters, including the putative monosaccharide transporter *SlSFP7*, with a role in sink tissues (García-Rodríguez et al. 2005), and the *PLASTID GLUCOSE TRANSLOCATOR 2*, orthologous to the *AtSGB1* glucose transporter, expressed in dividing cells (Wang et al. 2006), also points to linking the privation of carbohydrates with reduced root biomass.

Roots are major photoassimilate sinks, and less strength has been linked to less LR formation (Lambers, Atkin, and Millenaar 2002). Shoot-derived carbohydrate catabolism affects the translation of AUX-induced factors linked to LR formation via TOR signalling while having only a marginal effect on the AUX-induced transcriptional response (Stitz et al. 2023). Although photosynthetic sugars act as shoot-to-root signals that induce LR initiation in an AUX-tunable manner, carbohydrate-dependent root elongation can occur independently of AUX signalling (Kircher and Schopfer 2023). In MT-infected plants, although the transcriptional profiling of AUX-responsive genes did not fully account for the impaired LR development, the reduction in glucose/fructose levels, along with the repression of genes related to oligosaccharide, sucrose, and starch metabolism, as well as components of the TOR signalling pathway, may, at least partially, explain the limited root growth.

Shoot-infection of MT leads to limited ^{13}C content in roots. In contrast, no difference was observed in the roots of inoculated low CK *35S::AtCKX2* plants, which exhibit no significant increase in stem diameter (Costa et al. 2021) nor impairment in LR growth. The absence of symptoms does not create a sink at the site of infection (Paschoal et al. 2022), and, therefore, it might not contribute to physiological constraints or limit carbon supply to the roots. It is worth noting that the total foliar area of MT plants was reduced after infection (Figure S12b), possibly interfering with ^{13}C reallocation to the roots. These findings indicate that root impairment after MT infection is likely significantly affected by sugar deficiency, probably due to sink establishment at the site of infection or a reduced photosynthetic rate in leaves (Paschoal et al. 2022). It has been reported that infection of grapevine by the rust *Phakopsora euvitis* leads to decreased photosynthetic rates and hypertrophy of mesophyll cells around the infection site, limiting the carbohydrate supply to the roots (Nogueira Júnior et al. 2017).

Along with the downregulation of carbohydrate-related genes, a subset of genes involved in coenzyme (energy) metabolism and

cell respiration was repressed, particularly those associated with oxidative phosphorylation and glycolysis, which may be linked to the observed decrease in root biomass (Fernie, Carrari, and Sweetlove 2004). Under insufficient carbohydrate supply, proteins can be degraded, and amino acids can be used as alternative substrates for mitochondrial respiration/ATP production (Batista-Silva et al. 2019; Heinemann and Hildebrandt 2021). We identified the upregulation of genes involved in amino acid catabolism, including *SlBCAT6*, which acts in the recycling of proteolytically derived branched-chain amino acids (Maloney et al. 2010). The decrease in proline, leucine, valine, and lysine levels might contribute to ATP production, either by redirecting the carbon skeleton to the TCA cycle, as suggested by the significant increase in TCA cycle intermediates, and/or by transferring electrons into the respiratory chain (Hildebrandt et al. 2015; Dellero 2020).

The limitation of carbohydrates is also reflected in the downregulation of genes related to cell wall metabolism and polysaccharide biosynthesis in the roots of infected MT and in the reduction in polysaccharides and starch observed by histology of root cross-sections. The cell wall is an important carbon pool of the plant biomass, which reflects the carbon status (Schädel et al. 2010; Huang et al. 2021). In particular, the repression of lipid-transfer proteins, orthologous to glycosylphosphatidylinositol-anchored proteins in Arabidopsis, involved in cell wall regulation (Zhou 2022), and genes involved in pectin metabolism, such as β-galactosidases and pectin-acetyl esterase, which contribute to cell wall loosening and LR development (Prince et al. 2019; Wachsman et al. 2020), may account for the reduction in root growth. The accumulation of cell wall metabolite precursors (glucarate and galactonate) also suggests that incorporating precursors into polymers is not adequate (Chu et al. 2019).

We observed a reduction in the primary roots' diameter and xylem area, which may impair adequate water and/or nutrient uptake and transport (Lynch 2022). In agreement, roots of infected MT exhibited the upregulation of genes encoding tonoplast intrinsic proteins (aquaporins) and increased levels of trehalose, typically induced in response to water stress in plants (Bárzana and Carvajal 2020; Padilla et al. 2023). Furthermore, the induction of high-affinity nitrogen transporters may indicate nitrogen deprivation (Lezhneva et al. 2014; Krapp 2015), while the reduced levels of glutamine and asparagine suggest hydrolysis of their amide groups to remobilise nitrogen within the roots (Hildebrandt et al. 2015). Similarly, the upregulation of genes encoding phosphate transporters and the reduced content of organic phosphate suggests a scenario of phosphate starvation (Castrillo et al. 2017).

Altogether, our data reveal that the roots of infected MT by *M. perniciosa* undergo a transcriptional and metabolic rearrangement, probably as a result of restriction of sugar availability, decreasing local carbohydrate and amino acid levels leading to the repression of genes involved in root respiration and carbohydrate, amino acid, and cell wall metabolism (Figure S16). Reduction in LR growth might contribute to yield losses by *M. perniciosa* infection in MT (Paschoal et al. 2022). Future studies should investigate whether root reduction in cacao is similarly driven by sink competition, as excessive shoot outgrowth in witches' broom symptoms may compete for energy and carbon. The reduced starch content observed within cacao seedling roots could potentially affect the capacity for water and nutrient uptake and/or interaction with the rhizosphere microbiota. Belowground interactions in cacao agroforestry systems are less evident than aboveground interactions and remain primarily unexplored; here, we shed light on how *M. perniciosa* infection might chronically affect host root function.

Acknowledgements

This work was supported by the 'Fundação de Amparo à Pesquisa do Estado de São Paulo' (FAPESP) by a Thematic Research Grant (2016/10498-4) and fellowships to DP (2018/18711-4), and EMS (2017/17000-4). Additional support came from the National Research and Technological Council (CNPq) by the research grants to AF (471631/2013-2) and EMS (409681/2018) and scholarships to AF, PJPLT and RVR. The support from Bárbara Gonçalves, Lucas Melloto, Bruna Queiroz, Rafael Monteiro, and Rodolfo Maniero was greatly appreciated. We thank Dr. Roberto Fritsche Neto (ESALQ, USP) for granting access to WinRHIZO. We thank Matheus Vicente and Luis Damasceno for the fruitful discussions. We are grateful to Maria Helena Pereira for the help with the schematic model, to Pedro Carvalho for the support in submitting the sequence data and to João Geraldo Brancalion for helping with the figures. We thank Prof. Adriana P. Martinelli for granting access to the microscope facility. We thank the University of North Carolina High Throughput Sequencing Facility for the support with the RNA-seq analysis and the Universitat Politècnica de València for the support with the hormonal analysis. Research was supported by LNBR—Brazilian National Laboratory of Biorenewables (CNPEM/MCTIC) during the use of the Metabolomics open-access facility.

Conflicts of Interests

The authors declare no conflicts of interest.

Data Availability Statement

The data that support the findings of this study are openly available in NCBI SRA database (PRJNA1032597) at https://www.ncbi.nlm.nih.gov/sra.

References

Almeida, A. A., and R. R. Valle. 2010. "Cacao: Ecophysiology of Growth and Production." In *Ecophysiology of Tropical Tree Crops*, edited by Fábio da Matta, 37–70. Nova Science Publishers, Inc.

Bárzana, G., and M. Carvajal. 2020. "Genetic Regulation of Water and Nutrient Transport in Water Stress Tolerance in Roots." *Journal of Biotechnology* 324: 134–142.

Batista-Silva, W., B. Heinemann, N. Rugen, et al. 2019. "The Role of Amino Acid Metabolism During Abiotic Stress Release." *Plant, Cell and Environment* 42: 1630–1644.

Benjamini, Y., and Y. Hochberg. 1995. "Controlling the False Discovery Rate: A Practical and Powerful Approach to Multiple Testing." *Journal of the Royal Statistical Society Series B: Statistical Methodology* 57: 289–300.

Bosse, D., and M. Köck. 1998. "Influence of Phosphate Starvation on Phosphohydrolases During Development of Tomato Seedlings." *Plant, Cell, and Environment* 21: 325–332.

Carmona, C. P., C. G. Bueno, A. Toussaint, et al. 2021. "Fine-Root Traits in the Global Spectrum of Plant Form and Function." *Nature* 597: 683–687.

Castrillo, G., P. J. P. L. Teixeira, S. H. Paredes, et al. 2017. "Root Microbiota Drive Direct Integration of Phosphate Stress and Immunity." *Nature* 543: 513–518.

Chen, L. Q., X. Q. Qu, B. H. Hou, et al. 2012. "Sucrose Efflux Mediated by Sweet Proteins as a Key Step for Phloem Transport." *Science* 335: 207–211.

Chu, Q., Z. Sha, H. Maruyama, et al. 2019. "Metabolic Reprogramming in Nodules, Roots, and Leaves of Symbiotic Soybean in Response to Iron Deficiency." *Plant, Cell and Environment* 42: 3027–3043.

Costa, J. L., D. Paschoal, E. M. da Silva, et al. 2021. "*Moniliophthora perniciosa*, the Causal Agent of Witches' Broom Disease of Cacao, Interferes With Cytokinin Metabolism During Infection of Micro-tom Tomato and Promotes Symptom Development." *New Phytologist* 231: 365–381.

Crookshanks, M., G. Taylor, and L. Dolan. 1998. "A Model System to Study the Effects of Elevated Co_2 on the Developmental Physiology of Roots: The Use of *Arabidopsis thaliana*." *Journal of Experimental Botany* 49: 593–597.

Cuadros-Inostroza, Á., C. Caldana, H. Redestig, et al. 2009. "TargetSearch—A Bioconductor Package for the Efficient Preprocessing of GC-MS Metabolite Profiling Data." *BMC Bioinformatics* 10: 428.

Deganello, J., G. A. Leal, M. L. Rossi, L. E. P. Peres, and A. Figueira. 2014. "Interaction of *Moniliophthora perniciosa* Biotypes With Micro-Tom Tomato: A Model System to Investigate the Witches' Broom Disease of *Theobroma cacao*." *Plant Pathology* 63: 1251–1263.

Dellero, Y. 2020. "Manipulating Amino Acid Metabolism to Improve Crop Nitrogen Use Efficiency for a Sustainable Agriculture." *Frontiers in Plant Science* 11: 602548.

Devaux, C., P. Baldet, J. Joubès, et al. 2003. "Physiological, Biochemical and Molecular Analysis of Sugar-Starvation Responses in Tomato Roots." *Journal of Experimental Botany* 54: 1143–1151.

Dhandapani, P., J. Song, O. Novak, and P. E. Jameson. 2017. "Infection by *Rhodococcus fascians* Maintains Cotyledons as a Sink Tissue for the Pathogen." *Annals of Botany* 119: 841–852.

Dhaouadi, S., A. H. Mougou, and A. Rhouma. 2020. "The Plant Pathogen *Rhodococcus fascians*. History, Disease Symptomatology, Host Range, Pathogenesis and Plant–Pathogen Interaction." *Annals of Applied Biology* 177: 4–15.

Duque, L. O., and A. Villordon. 2019. "Root Branching and Nutrient Efficiency: Status and Way Forward in Root and Tuber Crops." *Frontiers in Plant Science* 10: 237.

Dutta, P., A. Kumari, M. Mahanta, et al. 2023. "Nanotechnological Approaches for Management of Soil-Borne Plant Pathogens." *Frontiers in Plant Science* 14: 1136233.

Feder, N., and T. P. O'Brien. 1968. "Plant Microtechnique: Some Principles and New Methods." *American Journal of Botany* 55: 123–142.

Fernie, A. R., F. Carrari, and L. J. Sweetlove. 2004. "Respiratory Metabolism: Glycolysis, the TCA Cycle and Mitochondrial Electron Transport." *Current Opinion in Plant Biology* 7: 254–261.

Franklin, G., and A. C. P. Dias. 2011. "Chlorogenic Acid Participates in the Regulation of Shoot, Root and Root Hair Development in *Hypericum perforatum*." *Plant Physiology and Biochemistry* 49: 835–842.

Fukushima, R. S., and M. S. Kerley. 2011. "Use of Lignin Extracted From Different Plant Sources as Standards in the Spectrophotometric Acetyl Bromide Lignin Method." *Journal of Agricultural and Food Chemistry* 59: 3505–3509.

García-Rodríguez, S., M. J. Pozo, C. Azcón-Aguilar, and N. Ferrol. 2005. "Expression of a Tomato Sugar Transporter Is Increased in Leaves of Mycorrhizal or *Phytophthora parasitica*-Infected Plants." *Mycorrhiza* 15: 489–496.

Giavalisco, P., Y. Li, A. Matthes, et al. 2011. "Elemental Formula Annotation of Polar and Lipophilic Metabolites Using ^{13}C, ^{15}N and ^{34}S Isotope Labelling, in Combination With High-Resolution Mass Spectrometry." *Plant Journal* 68: 364–376.

González-Hernández, A. I., L. Scalschi, P. García-Agustín, and G. Camañes. 2020. "Exogenous Carbon Compounds Modulate Tomato Root Development." *Plants* 9: 837.

Gorshkov, V., and I. Tsers. 2022. "Plant Susceptible Responses: The Underestimated Side of Plant–Pathogen Interactions." *Biological Reviews* 97: 45–66.

Gu, Z., R. Eils, and M. Schlesner. 2016. "Complex Heatmaps Reveal Patterns and Correlations in Multidimensional Genomic Data." *Bioinformatics* 32: 2847–2849.

Heinemann, B., and T. M. Hildebrandt. 2021. "The Role of Amino Acid Metabolism in Signaling and Metabolic Adaptation to Stress-Induced Energy Deficiency in Plants." *Journal of Experimental Botany* 72: 4634–4645.

Hemmati, C., M. Nikooei, and A. M. Al-Sadi. 2021. "*Candidatus* Phytoplasma aurantifolia Increased the Fitness of *Hishimonus phycitis*; The Vector of Lime Witches' Broom Disease." *Crop Protection* 142: 105532.

Hildebrandt, T. M., A. Nunes Nesi, W. L. Araújo, and H. P. Braun. 2015. "Amino Acid Catabolism in Plants." *Molecular Plant* 8: 1563–1579.

Huang, J., A. Hammerbacher, J. Gershenzon, et al. 2021. "Storage of Carbon Reserves in Spruce Trees Is Prioritized Over Growth in the Face of Carbon Limitation." *Proceedings of the National Academy of Sciences* 118: e2023297118.

Jensen, L. S., L. H. Merrill, C. V. Reddy, and J. McGinnis. 1962. "Observations on Eating Patterns and Rate of Food Passage of Birds Fed Pelleted and Unpelleted Diets." *Poultry Science* 41: 1414–1419.

Johansen, D. A. 1940. *Plant Microtechnique*, 530. London: McGraw-Hill Book Company, Inc.

Kircher, S., and P. Schopfer. 2023. "Photosynthetic Sucrose Drives the Lateral Root Clock in Arabidopsis Seedlings." *Current Biology* 33: 2201–2212.e3.

Kocal, N., U. Sonnewald, and S. Sonnewald. 2008. "Cell Wall-Bound Invertase Limits Sucrose Export and Is Involved in Symptom Development and Inhibition of Photosynthesis During Compatible Interaction Between Tomato and *Xanthomonas campestris* pv *vesicatoria*." *Plant Physiology* 148: 1523–1536.

Krapp, A. 2015. "Plant Nitrogen Assimilation and Its Regulation: A Complex Puzzle With Missing Pieces." *Current Opinion in Plant Biology* 25: 115–122.

Kummerow, J., M. Kummerow, and W. Souza da Silva. 1982. "Fine-Root Growth Dynamics in Cacao (*Theobroma cacao*)." *Plant and Soil* 65: 193–201.

Lambers, H., O. K. Atkin, and F. F. Millenaar. 2002. "Respiratory Patterns In Roots In Relation to Their Functioning." In *Plant Roots: The Hidden Half*, edited by Waisel, A. Eshel, and K. Kafkaki, 521–552. New York: Marcel Dekker, Inc.

Lezhneva, L., T. Kiba, A. B. Feria-Bourrellier, et al. 2014. "The Arabidopsis Nitrate Transporter Nrt 2.5 Plays a Role in Nitrate Acquisition and Remobilization in Nitrogen-Starved Plants." *Plant Journal* 80: 230–241.

Li, G., and Y. Zhao. 2024. "The Critical Roles of Three Sugar-Related Proteins (Hxk, SnRK1, TOR) in Regulating Plant Growth and Stress Responses." *Horticulture Research* 11, no. 6. https://doi.org/10.1093/hr/uhae099.

Li, H., C. Testerink, and Y. Zhang. 2021. "How Roots and Shoots Communicate Through Stressful Times." *Trends in Plant Science* 26: 940–952.

Lisboa, D. O., H. C. Evans, J. P. M. Araújo, S. G. Elias, and R. W. Barreto. 2020. "*Moniliophthora perniciosa*, the Mushroom Causing Witches' Broom Disease of Cacao: Insights Into Its Taxonomy, Ecology and Host Range in Brazil." *Fungal Biology* 124: 983–1003.

Liu, J., L. Han, B. Huai, et al. 2015. "Down-Regulation of a Wheat Alkaline/Neutral Invertase Correlates With Reduced Host Susceptibility to Wheat Stripe Rust Caused by *Puccinia striiformis*." *Journal of Experimental Botany* 66: 7325–7338.

Lynch, J. P. 2022. "Harnessing Root Architecture to Address Global Challenges." *Plant Journal* 109: 415–431.

Maloney, G. S., A. Kochevenko, D. M. Tieman, et al. 2010. "Characterization of the Branched-Chain Amino Acid Aminotransferase Enzyme Family in Tomato." *Plant Physiology* 153: 925–936.

Marelli, J. P., S. N. Maximova, K. P. Gramacho, S. Kang, and M. J. Guiltinan. 2009. "Infection Biology of *Moniliophthora perniciosa* on *Theobroma cacao* and Alternate Solanaceous Hosts." *Tropical Plant Biology* 2: 149–160.

Marhavý, P., M. Vanstraelen, B. De Rybel, et al. 2012. "Auxin Reflux Between the Endodermis and Pericycle Promotes Lateral Root Initiation." *EMBO Journal* 32: 149–158.

Martínez-Bello, L., T. Moritz, and I. López-Díaz. 2015. "Silencing C19-GA 2-oxidases Induces Parthenocarpic Development and Inhibits Lateral Branching in Tomato Plants." *Journal of Experimental Botany* 66: 5897–5910.

McCormack, M. L., I. A. Dickie, D. M. Eissenstat, et al. 2015. "Redefining Fine Roots Improves Understanding of Below-Ground Contributions to Terrestrial Biosphere Processes." *New Phytologist* 207: 505–518.

McIntyre, K. E., D. R. Bush, and C. T. Argueso. 2021. "Cytokinin Regulation of Source-Sink Relationships in Plant-Pathogen Interactions." *Frontiers in Plant Science* 12: 677585.

Morales-Herrera, S., J. Jourquin, F. Coppé, et al. 2023. "Trehalose-6-phosphate Signaling Regulates Lateral Root Formation in *Arabidopsis thaliana*." *Proceedings of the National Academy of Sciences* 120: e2302996120.

Motte, H., S. Vanneste, and T. Beeckman. 2019. "Molecular and Environmental Regulation of Root Development." *Annual Review of Plant Biology* 70: 465–488.

Muller, B., Y. Guédon, S. Passot, et al. 2019. "Lateral Roots: Random Diversity in Adversity." *Trends in Plant Science* 24: 810–825.

Muñoz, F., and J. Beer. 2001. "Fine Root Dynamics of Shaded Cacao Plantations in Costa Rica." *Agroforestry Systems* 51: 119–130.

Nogueira Júnior, A. F., R. V. Ribeiro, B. Appezzato-da-Glória, M. K. M. Soares, J. B. Rasera, and L. Amorim. 2017. "*Phakopsora euvitis* Causes Unusual Damage to Leaves and Modifies Carbohydrate Metabolism in Grapevine." *Frontiers in Plant Science* 8: 1675.

Noorizadeh, S., R. Khakvar, and M. Golmohammadi. 2022. "Effect of Temperature on Symptom Expression of Witches' Broom Disease in Commercial Citrus Species." *Tropical Plant Pathology* 47: 278–286.

Oh, K., M. G. Ivanchenko, T. J. White, and T. L. Lomax. 2006. "The *Diageotropica* Gene of Tomato Encodes a Cyclophilin: A Novel Player in Auxin Signaling." *Planta* 224: 133–144.

Padilla, Y. G., R. Gisbert-Mullor, E. Bueso, et al. 2023. "New Insights into Short-Term Water Stress Tolerance Through Transcriptomic and Metabolomic Analyses on Pepper Roots." *Plant Science* 333: 111731.

Paredes, S. H. 2016. AMOR 0.0-14. Zenodo. https://doi.org/10.5281/zenodo.49093.

Paschoal, D., J. L. Costa, E. M. da Silva, et al. 2022. "Infection by *Moniliophthora perniciosa* Reprograms Tomato 'Micro-Tom' Physiology, Establishes a Sink, and Increases Secondary Cell Wall Synthesis." *Journal of Experimental Botany* 73: 3651–3670.

Perianez-Rodriguez, J., M. Rodriguez, M. Marconi, et al. 2021. "An Auxin-Regulable Oscillatory Circuit Drives the Root Clock in Arabidopsis." *Science Advances* 7: eabd4722.

Pino, L. E., J. E. Lima, M. H. Vicente, et al. 2022. "Increased Branching Independent of Strigolactone in Cytokinin Oxidase 2-Overexpressing Tomato Is Mediated by Reduced Auxin Transport." *Molecular Horticulture* 2: 12.

Pino, L. E., S. Lombardi-Crestana, M. S. Azevedo, et al. 2010. "The Rg1 Allele as a Valuable Tool for Genetic Transformation of the Tomato 'Micro-Tom' Model System." *Plant Methods* 6: 23.

Prince, S. J., B. Valliyodan, H. Ye, et al. 2019. "Understanding Genetic Control of Root System Architecture in Soybean: Insights Into the Genetic Basis of Lateral Root Number." *Plant, Cell and Environment* 42: 212–229.

Purdy, L., and R. Schmidt. 1996. "Status of Cacao Witches' Broom: Biology, Epidemiology, and Management." *Annual Review of Phytopathology* 34: 573–594.

R Core Team. 2020. *R: A Language and Environment for Statistical Computing*. Vienna, Austria: R Foundation for Statistical Computing. https://www.R-project.org/.

Raiesi, T., and M. Golmohammadi. 2020. "Changes in Nutrient Concentrations and Biochemical Characteristics of Mexican Lime (*Citrus aurantifolia*) Infected by Phytoplasma." *Journal of General Plant Pathology* 86: 486–493.

Reyes-Hernández, B. J., and A. Maizel. 2023. "Tunable Recurrent Priming of Lateral Roots in Arabidopsis: More Than Just a Clock?" *Current Opinion in Plant Biology* 76: 102479.

Robinson, M. D., D. J. McCarthy, and G. K. Smyth. 2010. "edgeR: A Bioconductor Package for Differential Expression Analysis of Digital Gene Expression Data." *Bioinformatics* 26: 139–140.

Rogers, E. D., and P. N. Benfey. 2015. "Regulation of Plant Root System Architecture: Implications for Crop Advancement." *Current Opinion in Biotechnology* 32: 93–98.

Sakai, W. S. 1973. "Simple Method for Differential Staining of Paraffin Embedded Plant Material Using Toluidine Blue O." *Stain Technology* 48: 247–249.

Schädel, C., A. Richter, A. Blöchl, and G. Hoch. 2010. "Hemicellulose Concentration and Composition in Plant Cell Walls Under Extreme Carbon Source–Sink Imbalances." *Physiologia Plantarum* 139: 241–255.

Silva, S. F., M. T. Miranda, V. E. Costa, E. C. Machado, and R. V. Ribeiro. 2021. "Sink Strength of Citrus Rootstocks Under Water Deficit." *Tree Physiology* 41: 1372–1383.

Stacklies, W., H. Redestig, M. Scholz, D. Walther, and J. Selbig. 2007. "Pcamethods—A Bioconductor Package Providing PCA Methods for Incomplete Data." *Bioinformatics* 23: 1164–1167.

Stamler, R. A., J. Kilcrease, C. Kallsen, et al. 2015. "First Report of *Rhodococcus* Isolates Causing Pistachio Bushy Top Syndrome on 'UCB-1'rootstock in California and Arizona." *Plant Disease* 99: 1468–1476.

Stitz, M., D. Kuster, M. Reinert, et al. 2023. "TOR Acts as a Metabolic Gatekeeper for Auxin-Dependent Lateral Root Initiation in *Arabidopsis thaliana*." *EMBO Journal* 42: e111273.

Thimm, O., O. Bläsing, Y. Gibon, et al. 2004. "MAPMAN: A User-Driven Tool to Display Genomics Data Sets Onto Diagrams of Metabolic Pathways and Other Biological Processes." *Plant Journal* 37: 914–939.

Torres-Martínez, H. H., S. Napsucialy-Mendivil, and J. G. Dubrovsky. 2022. "Cellular and Molecular Bases of Lateral Root Initiation and Morphogenesis." *Current Opinion in Plant Biology* 65: 102115.

Vermeer, J. E. M., D. von Wangenheim, M. Barberon, et al. 2014. "A Spatial Accommodation by Neighboring Cells Is Required for Organ Initiation in Arabidopsis." *Science* 343: 178–183.

Silva, N.V., P. Mazzafera, and I. Cesarino. 2019. "Should I Stay or Should I Go: Are Chlorogenic Acids Mobilized Towards Lignin Biosynthesis?" *Phytochemistry* 166: 112063.

Wachsman, G., J. Zhang, M. A. Moreno-Risueno, C. T. Anderson, and P. N. Benfey. 2020. "Cell Wall Remodeling and Vesicle Trafficking Mediate the Root Clock in Arabidopsis." *Science* 370: 819–823.

Wang, H. X., R. R. Weerasinghe, T. D. Perdue, et al. 2006. "A Golgi-Localized Hexose Transporter Is Involved in Heterotrimeric G Protein-Mediated Early Development in Arabidopsis." *Molecular Biology of the Cell* 17: 4257–4269.

Wang, M. B., and Q. Zhang. 2009. "Issues in Using the WinRHIZO System to Determine Physical Characteristics of Plant Fine Roots." *Acta Ecologica Sinica* 29: 136–138.

Wang, Y., H. Zhao, L. Xu, et al. 2023. "PUB30-mediated Down-regulation of the HB24-SWEET11 Module Is Involved in Root Growth Inhibition Under Salt Stress by Attenuating Sucrose Supply in Arabidopsis." *New Phytologist* 237: 1667–1683.

Werner, T., V. Motyka, V. Laucou, R. Smets, H. Van Onckelen, and T. Schmülling. 2003. "Cytokinin-Deficient Transgenic Arabidopsis Plants Show Multiple Developmental Alterations Indicating Opposite Functions of Cytokinins in the Regulation of Shoot and Root Meristem Activity." *Plant Cell* 15: 2532–2550.

Yu, G., L. G. Wang, Y. Han, and Q. Y. He. 2012. "Clusterprofiler: An R Package for Comparing Biological Themes Among Gene Clusters." *OMICS: A Journal of Integrative Biology* 16: 284–287.

Yu, S. M., S. F. Lo, and T. H. D. Ho. 2015. "Source–Sink Communication: Regulated by Hormone, Nutrient, and Stress Cross-Signaling." *Trends in Plant Science* 20: 844–857.

Zhang, J., R. Chen, J. Xiao, et al. 2007. "A Single-Base Deletion Mutation in SlIAA9 Gene Causes Tomato (*Solanum lycopersicum*) *entire* Mutant." *Journal of Plant Research* 120: 671–678.

Zhang, Y., Y. Ma, D. Zhao, et al. 2023. "Genetic Regulation of Lateral Root Development." *Plant Signaling and Behavior* 18: 2081397.

Zhou, K. 2022. "The Regulation of the Cell Wall by Glycosylphosphatidylinositol-Anchored Proteins in Arabidopsis." *Frontiers in Cell and Developmental Biology* 10: 904714.

Supporting Information

Additional supporting information can be found online in the Supporting Information section.